Desalination and Water Treatment
www.deswater.com
doi: 10.5004/dwt.2020.26267

204 (2020) 297–305
November

Removal of chromium(III) ions from aqueous solutions using different types of hydroxyapatites

Inga Zinicovscaia[a,b,c,*], Nikita Yushin[a], Dmitrii Grozdov[a], Ionel Humelnicu[d], Doina Humelnicu[d], Tatiana Mitina[c]

[a]*Joint Institute for Nuclear Research, Joliot-Curie Str., 6, 1419890 Dubna, Russia, Tel. +74962163653; Fax: +74962165085; emails: zinikovskaia@mail.ru (I. Zinicovscaia), ynik_62@mail.ru (N. Yushin), dsgrozdov@rambler.ru (D. Grozdov)*
[b]*Horia Hulubei National Institute for R&D in Physics and Nuclear Engineering, 30 Reactorului Str. MG-6, Bucharest - Magurele, Romania*
[c]*The Institute of Chemistry, 3, Academiei Str., 2028 Chisinau, R. Moldova, email: mitina_tatiana@mail.ru (T. Mitina)*
[d]*"Alexandru Ioan Cuza" University of Iasi, Faculty of Chemistry, Iasi, Romania, emails: ionel@uaic.ro (I. Humelnicu), doinah@uaic.ro (D. Humelnicu)*

Received 20 January 2020; Accepted 9 June 2020

ABSTRACT

This study explored the possibility of using hydroxyapatite and its two modifications as sorbents to remove Cr(III) ions under different experimental conditions. The effect of pH (3–7), chromium concentration (10–100 mg L^{-1}) and time (5–60 min) on adsorption was investigated. The Langmuir, Freundlich and Temkin adsorption models were applied to describe experimental data. Maximum adsorption capacity constituted 78.1 mg g^{-1} for hydroxyapatite treated with pluronic P123, 79.7 mg g^{-1} for hydroxyapatite and 134 mg g^{-1} for hydroxyapatite treated with pluronic F127 surfactant. The pseudo-first-order, pseudo-second-order, Elovich and intraparticle diffusion models were used to describe the kinetics of the process. For all sorbents, the experimental data fitted very well the pseudo-second-order and intraparticle diffusion models. The obtained results showed the potential of synthesized sorbents to be used for Cr(III) removal from wastewater.

Keywords: Chromium(III); Adsorption; Hydroxyapatite; Flame atomic adsorption spectrometry

1. Introduction

Water contamination caused by heavy metals deserves increasing attention in many counties today, mainly due to their high toxicity, non-biodegradable nature and high accumulation capacity [1]. Conventional techniques of heavy metal removal from industrial effluents include precipitation, flocculation, filtration, evaporation, solvent extraction, sorption, ion-exchange, electrodialysis, and membrane separation processes [2,3]. Often these techniques are expensive or ineffective at metal concentrations in solution less than 100 mg L^{-1} [4]. Thus, there is a great need to develop cheap and eco-friendly techniques for environmental remediation. Adsorption has been considered as one of the most efficient methods because of the possibility to archive high removal efficiency and its low operation cost [1]. The hydroxyapatite is an ideal sorbent for long-term containment of contaminants because of its high adsorption capacity, low water solubility, high stability under reducing and oxidizing conditions, good thermal stability, availability, and low cost [5,6]. Hydroxyapatite has a high removal capacity, mainly for divalent heavy metal ions and has been used for wastewater treatment [5–8].

Among the toxic heavy metal species present in the environment, chromium pollution of the water resources is a major problem because of the high toxicity of its compounds.

* Corresponding author.

Cr(VI) is considered as the most toxic chromium species, however, Cr(III) is even considered as an important microelement for biochemical processes that can be converted in Cr(VI) under oxidative conditions, thus representing a potential risk for the environment and human health. In addition, chromium is prevalently introduced in the environment from anthropogenic sources in form of Cr(III) ions. Chromium(III) is released in water bodies from all the industrial activities involving the manufacturing or the application of metal alloys, metalliferous mining, electroplating, batteries, paints and pigments production, landfill leachate, electronics, manures sewage sludge, paper and pulp industry, and petroleum refinement [6,9,10].

The objective of this study was to test hydroxyapatite and two modifications of it as alternative adsorbent materials for the removal of Cr(III) ions from aqueous solutions. The effect of contact time, initial concentration, and pH on Cr(III) adsorption was investigated. Equilibrium and kinetic studies were performed in order to describe the adsorption process.

2. Materials and methods

Calcium nitrate, chromium nitrate and phosphoric acid as well as surfactants (pluronic P123 and pluronic F127) were purchased from Sigma-Aldrich (Germany). Ethylic alcohol and liquid ammonia were purchased from Chemical Company. All chemicals were reagent grade and were used without further purification.

2.1. Sorbents synthesis

Hydroxyapatite (HAP) was prepared by co-precipitation of calcium nitrate and phosphoric acid according to the synthesis reported by Arsad et al. [11] with some modifications. An aqueous solution of 0.5 M calcium nitrate was added to 50 mL ethanol and was vigorously stirred at room temperature. The pH of the solution was adjusted to 10 by addition of 25% (v/v) ammonia in the solution. The 0.3 M phosphoric acid was added slowly in a dropwise manner to allow reacting with calcium nitrate. After 1 h reaction at 60°C, the reaction mixture was kept to age overnight at room temperature to complete the reaction. Then, the suspension was centrifuged at 4,000 rpm for 15 min, separated and dried at room temperature. The white powder of the sample was calcined for 6 h at 550°C and labeled as HAP.

$$10\mathrm{Ca}\left(\mathrm{NO}_3\right)_2 + 6\mathrm{H}_3\mathrm{PO}_4 + 2\mathrm{H}_2\mathrm{O} \rightarrow \mathrm{Ca}_{10}\left(\mathrm{PO}_4\right)_6 + 20\mathrm{NHO}_3 \quad (1)$$

The HAP P123 and HAP F127 sorbents were obtained following the same procedure except that the corresponding surfactants were added to the reaction mixture. Thus, the pluronic P123 was used to synthesize HAP P123 sample, and pluronic F127 to synthesize HAP F127.

2.2. Adsorption experiments

The adsorption experiments were performed placing 0.02 g of sorbent in a 50 mL flask with 10 mL of a solution containing chromium at constant agitation. To determine the adsorption capacity of sorbents the effect of pH (3.0–7.0), time (5–60 min), Cr(III) concentration (10–100 mg L^{-1}) on chromium adsorption from batch solutions was studied. After experiments, the sorbent was separated from the solution by filtration and chromium concentration in the solution was determined. Experiments were performed in triplicate and the average of measurements was used in the calculation.

The chromium uptake q was calculated using the following equation:

$$q = \frac{V\left(C_i - C_f\right)}{m} \quad (2)$$

and adsorption removal efficiency, R (%) from the equation:

$$R = \frac{C_i - C_f}{C_i} \times 100 \quad (3)$$

where q is the amount of metal ions adsorbed on the sorbent, mg g^{-1}; V is the volume of solution, L; C_i is the initial concentration of metal in mg L^{-1}, C_f is the final metal concentration in the solution, mg L^{-1}, and m is the mass of sorbent, g.

2.3. Methods

The N_2 adsorption/desorption isotherms for Brunauer–Emmett–Teller specific surface area measurements were recorded on a NOVA 2200e (Quantachrome Instruments, USA) automated gas adsorption analyzer. Before analysis, the samples were outgassed at 120°C for at least 6 h under vacuum.

Chromium concentration in solution was determined at a resonance line of 357.9 nm by applying flame atomic absorption spectrometer (Kvant-2, Russia). The calibration solutions were prepared from a 1 g L^{-1} chromium stock solution (Atomic Absorption Spectroscopy standard solution; Merck, Germany). Infrared spectra were recorded in the range of 4,000–400 cm^{-1} using a Bruker Alpha Platinum-ATR spectrometer (Bruker Optics, Ettingen, Germany).

3. Results and discussion

3.1. Sorbents characterization

Nitrogen adsorption–desorption analysis was performed in order to characterize the porous structure of the synthesized sorbents. Fig. 1 shows typical isotherms characteristic to HAPs. According to the International Union of Pure and Applied Chemistry classification, the obtained isotherm obey type IV, containing hysteresis loops, which indicates the presence of mesopores in the adsorbent structure.

The textural characteristics of the investigated sorbents are presented in Table 1. The obtained data show that the addition of the surfactant P123 leads to a significant increase of specific surface area and total pore volume of the HAP in comparison with untreated HAP. With the addition of F127, the pore volume remains almost on the level of untreated HAP, while the specific surface area was reduced.

Fig. 2 represents the control of Fourier-transform infrared spectroscopy (FTIR) of HAP and its two modifications.

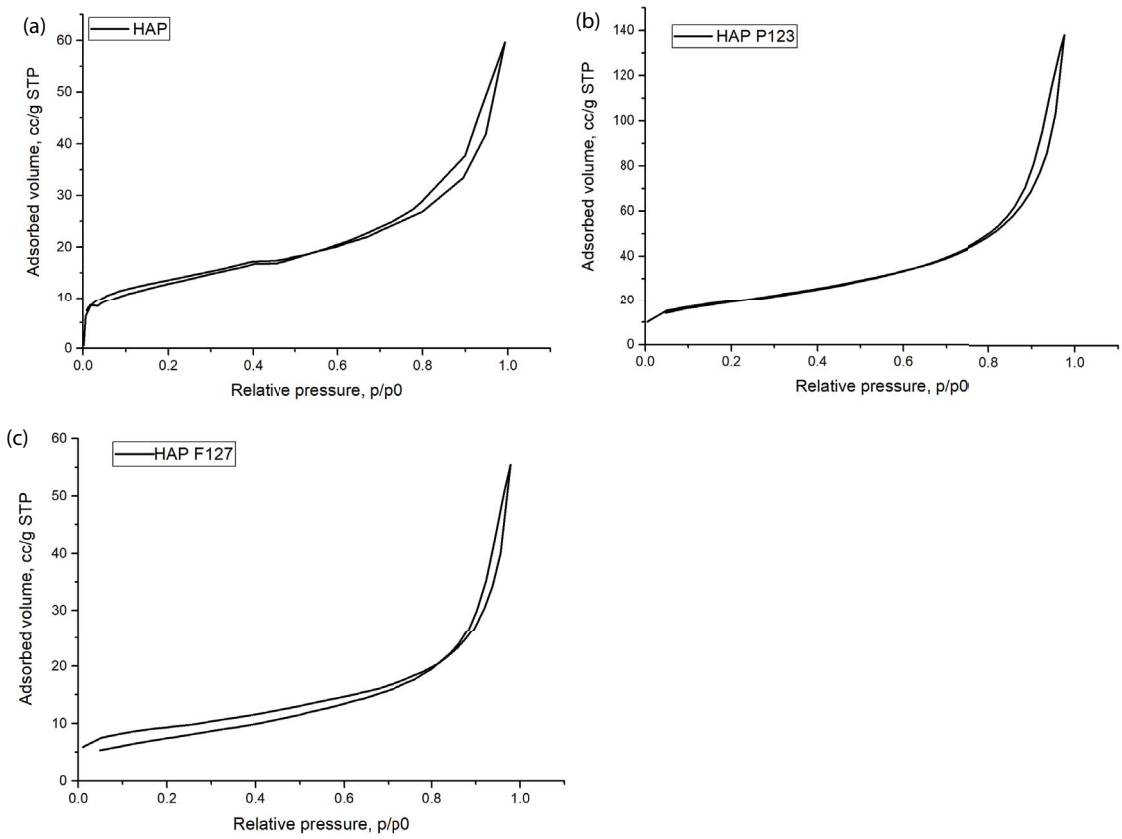

Fig. 1. Nitrogen adsorption isotherm and corresponding pore size distributions for the synthesized HAP samples (a) HAP, (b) HAP P123 and (c) HAP F127.

Table 1
Textural properties of the synthesized sorbents

Sorbent	Specific surface, m^2/g	Pore volume, cm^3/g	Pore diameter, nm
HAP	47.251	$6.48 \cdot 10^{-2}$	3.12
HAP P123	69.153	$1.59 \cdot 10^{-1}$	3.50
HAP F127	31.719	$6.18 \cdot 10^{-2}$	4.13

The FTIR spectra of the sorbents show characteristic bands due to presence of PO_4^{3-} ions (ν_1 – 963 cm^{-1}, ν_2 – 870 cm^{-1}, ν_3 – 1,036 and 1,095 cm^{-1}, ν_4 – 568 and 600 cm^{-1}) [12]. In the structure of HAP are bounded hydroxyl functional groups but the presence of stretching vibration of HO^- groups were not revealed by FTIR analysis. It could be caused by the ionic bond of HO^- groups or as a result of interference bonds due to the symmetry of molecules. In FTIR spectra of HAP P123 and HAP F127 was observed a slight increase in the intensity of deformation bands of PO_4^{3-} ions.

In the infrared spectra of Cr-loaded sorbents was observed the shifting of bands positions of PO_4^{3-} ions and change of frequencies (Fig. 3), which indicates their involvement in chromium ions binding.

The reduction of the intensity of PO_4^{3-} bands can be associated with the Cr(III) ions exchange with the protons and Ca(II) ions present on the HAP surface and coordination of Cr(III) with PO_4^{3-} [3,9]. This finding was supported by Deydier et al. [13], who found that Cr(III) ions binding to hydroxyapatite involves three successive steps: surface complexation of Cr(III) ions, HAP dissolution followed by $Cr_{20}((PO_4)_6(OH)_2)_3$ precipitation and slow metal diffusion/substitution of Ca(II) ions.

3.2. Effect of pH dependence of adsorption process

The effect of initial solution pH on Cr(III) removal was studied in the pH range 3.0–7.0. Experiments were not performed at pH < 3.0 since the removal of cations can be limited by electrostatic repulsion between the positively charged surface of the sorbent and cations [14]. According to data presented in Fig. 4 the highest Cr(III) removal was achieved at pH 5.0 for HAP and HAP P123: 97% and 97.6%, respectively. Maximum Cr(III) removal by HAP F127 was reached at pH 6.0 (98%). Even at pH 3.0 Cr(III), removal was not lower than 60%. According to Leyva-Ramos et al. [15] Cr(III) in dependence of the pH exists in the solutions in different forms: the predominant species below pH 2 is Cr^{3+} and between pH 6.5 and 10 the predominant species is $Cr(OH)_3$. At pH 3 Cr^{3+} (90%) and $CrOH^{2+}$ (10%) at pH 3. At pH 4, Cr(III) is present in solution in the form of Cr^{3+} (40%) and $Cr(OH)^{2+}$ (60%), at pH 5 in the form of $Cr(OH)^{2+}$ (70%) and $Cr_3(OH)_4^{5+}$ (20%) and at pH 6 $Cr(OH)^{2+}$ (40%), $Cr(OH)_2^+$ (35%) and $Cr_3(OH)_4^{5+}$ (25%).

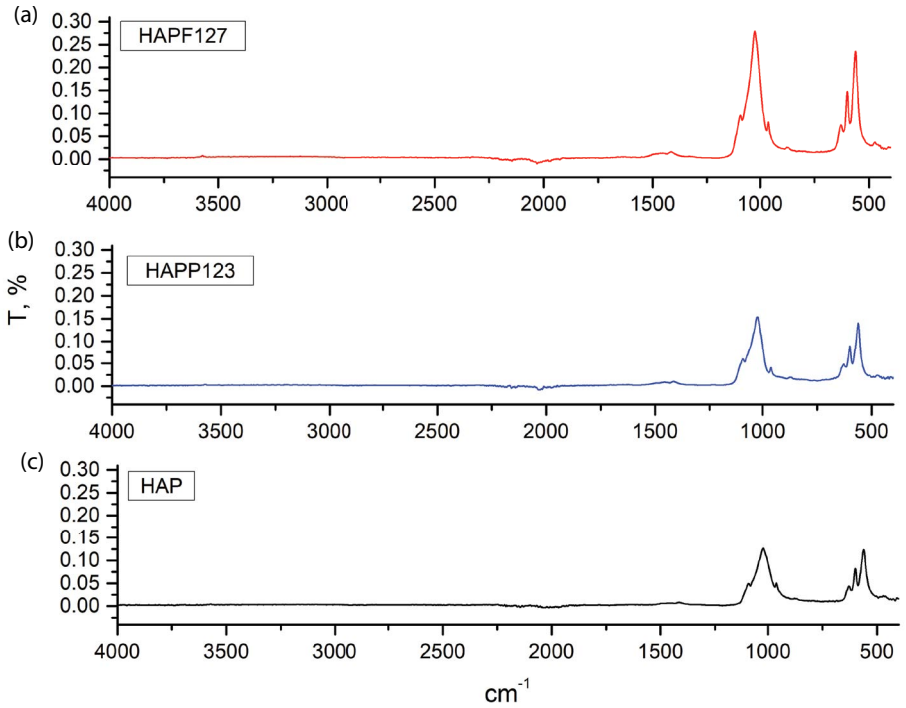

Fig. 2. FTIR spectra of (a) HAP, (b) HAP P123 and (c) HAP F127 control samples.[TS: Label (a), (b), (c) from bottom to top]

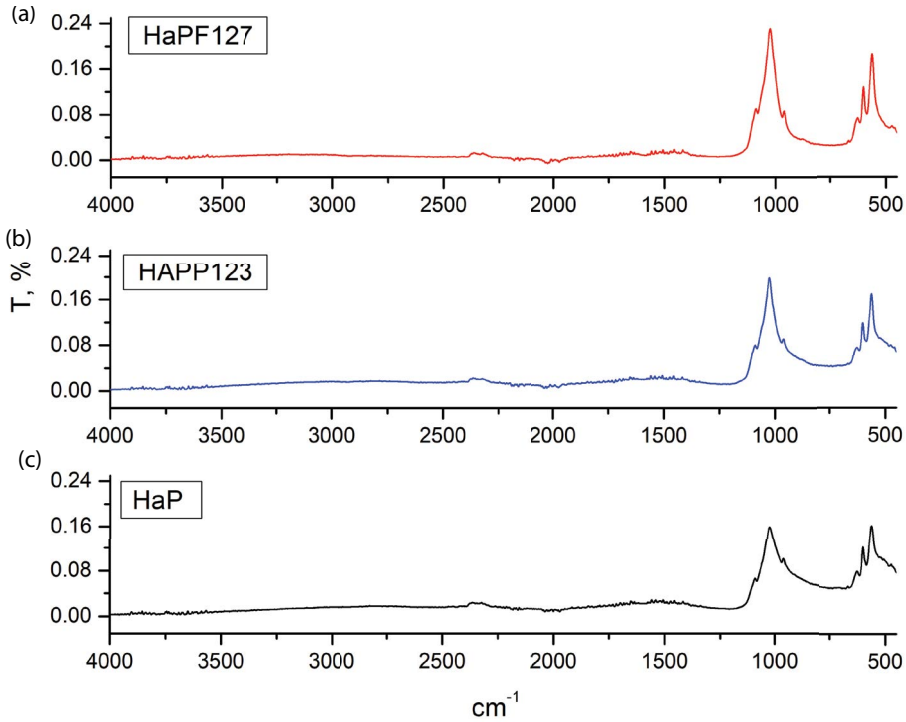

Fig. 3. FTIR spectra of Cr-loaded sorbents (a) HAP, (b) HAP P123 and (c) HAP F127

Wakamura et al. [16] in their study proposed two mechanisms of Cr(III) ions adsorption on the HAP (i) cation-exchange with Ca(II) ion or (ii) anion exchange with H_2PO^{4-} ions. It should be mentioned that anion exchange was possible at pH > 8 when chromium is present in solution in the $Cr(OH)^{4-}$ form. Maximum removal efficiency at pH 5–6, where chromium(III) is present in solution in the form of Cr^{3+}, $CrOH_2^+$ and $Cr_3(OH)_4^{5+}$ suggests that cation-exchange is the main mechanism of Cr(III) ions adsorption by HAP and its two modifications. Ferri et al. [6] showed that the mechanism of Cr-trapping on HAP surface at pH 4–6 is surface complexation or ionic exchange.

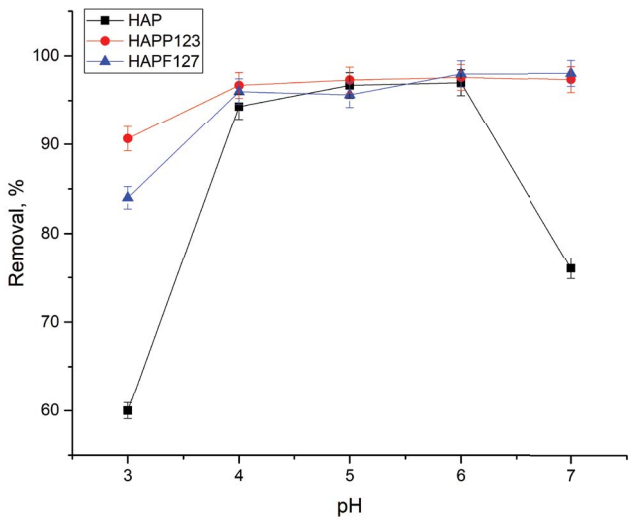

Fig. 4. Removal of chromium ions at different initial pH (temperature of 20°C; sorbent dosage 0.02 g; adsorption time 1 h).

3.3. Effect of contact time on the adsorption process

Contact time between adsorbent and adsorbed is related to the period needed for the establishment of the equilibrium within the adsorption system. The effect of contact time on the adsorption of Cr(III) ions on the three sorbents was studied in a range of 0–60 min. For all studied sorbents the equilibrium was achieved in 45 min when 89% of Cr(III) was removed by HAP, 97% by HAP P123 and 96% by HAP F127 (Fig. 5).

Contact time between adsorbent and adsorbate helps the understanding of adsorption kinetics since it provides important information with regard to mechanisms that control the adsorption process. The adsorption kinetic data were analyzed using the four most common kinetic models, namely, pseudo-first-order, pseudo-second-order, Elovich and intraparticle diffusion models. The models are expressed by the following formulas:

Pseudo-first-order model:

$$\log\left(q_e - q_t\right) = \log q_e - \frac{k_1}{2.303}t \tag{4}$$

where q_e and q_t are the amounts of chromium(III) (mg g^{-1}) adsorbed at equilibrium and at t (min) time, respectively, and k_1 (min^{-1}) is the rate constant of pseudo-first-order.

Pseudo-second-order model:

$$\frac{t}{q} = \frac{1}{k_2 q_e^2} + \frac{t}{q_e} \tag{5}$$

where k_2 (g mg^{-1} min^{-1}) is the rate constant of second-order.

Elovich model:

$$q_t = \frac{1}{\beta}\ln\left(\alpha\beta\right) + \frac{1}{\beta}\ln\left(t\right) \tag{6}$$

where α and β are the Elovich equation constants.

Weber and Morris intraparticle diffusion model:

$$q = k_{\text{diff}} \cdot t^{0.5} + C_i \tag{7}$$

where k_{diff} is the intraparticle diffusion rate constant (mg g^{-1} min$^{-1/2}$), C_i is the intercept, giving an idea about the thickness of the boundary layer.

The experimental kinetic data were described according to the indicated models (Fig. 6) and the coefficients of determination, as well as the kinetic parameters of Cr(III) adsorption on studied sorbents, are given in Table 2.

The coefficients of determination (R^2) show that the experimental results for Cr(III) ions on all analyzed sorbents are well described by the pseudo-second-order kinetic model. The pseudo-second-order model is based on the assumption that the rate-limiting step of the adsorption may be chemical adsorption or chemisorption involving valency forces through sharing or exchange of electrons between sorbent and sorbate [17]. The pseudo-second-order adsorption kinetics well fit-ted the adsorption of Cr(III), ions on HAP nanoparticles [3]. For Elovich and the pseudo-first-order model, the coefficient of determination values was significantly lower.

The intraparticle diffusion often plays an important role in the adsorption process when adsorbent is porous materials since it allows us to predict the rate-controlling step. In case when the plot of q_t vs. $t^{1/2}$ is linear and the line pass through the origin then intraparticle diffusion is considered the rate-controlling step. If the plot does not pass through the origin is an indication that the intraparticle diffusion is not the only rate-limiting step, but also other kinetic models may control the rate of adsorption, all of which may be operating simultaneously [18]. From Fig. 7 it is seen that there are three stages of Cr(III) adsorption (i) the first linear sharp region might due to the instantaneous adsorption of Cr(III) ions on the external surface of adsorbent; (ii) the second phase is the gradual adsorption phase, where the intraparticle diffusion is a rate-limiting step and (iii) the third

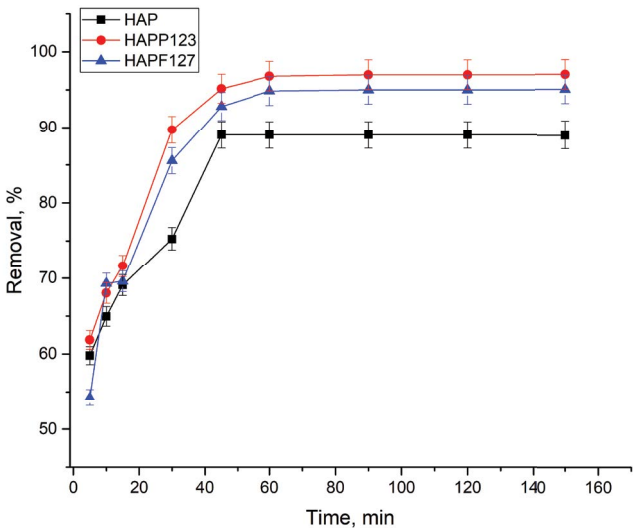

Fig. 5. Adsorption of chromium ions as the function of time (temperature 20°C; sorbent dosage 0.02 g).

Table 2
Kinetic parameters of the adsorption of chromium(III) ions

Kinetic model	Sorbent		
	HAP	HAP F127	HAP P123
Pseudo-first-order			
$q_{e,\text{exp.}}$ (mg g^{-1})	4.3	4.6	4.6
$q_{e,\text{cal.}}$ (mg g^{-1})	1.6	2.6	2.7
k_1 (min^{-1})	0.03	0.1	0.06
R^2	0.98	0.94	0.94
Pseudo-second-order			
$q_{e,\text{exp.}}$ (mg g^{-1})	4.3	4.6	4.6
$q_{e,\text{cal.}}$ (mg g^{-1})	4.4	4.8	4.85
k_2 (g mg^{-1} min^{-1})	0.28	0.25	0.28
R^2	0.998	0.999	0.999
Elovich model			
α (g mg^{-1} min^{-1})	44.4	24.6	14.1
β (g mg^{-1})	2.1	1.67	1.72
R^2	0.89	0.88	0.88
Intraparticle diffusion (for linear stage)			
k_{diff} (mg g^{-1} min$^{-1/2}$)	0.37	0.35	0.33
C_1	2.3	2.1	2.3
R^2	0.96	0.94	0.95

region is attributed to the final equilibrium stage where the adsorption process starts to slow down due to the high affinity of adsorbate adsorbed on the adsorbent surface [19].

Since the plot of q_t vs. $t^{1/2}$ did not pass through the origin for any of the phases (Fig. 7) it can be suggested that the intraparticle diffusion is not the only rate-controlling step. The positive value of C_i obtained for all sorbents depicts boundary layer effects [20].

3.4. Effect of the initial concentration of Cr(III) ions on the adsorption process

The adsorption of Cr(III) ions was carried out at Cr(III) concentration in the solution ranging from 10 to 100 mg L^{-1}. As it is shown in Fig. 8 adsorption capacity of sorbents increases with the increase of Cr(III) concentration in solution.

A higher initial concentration provides an important driving force to overcome all mass transfer resistances of the pollutant between the aqueous and solid phases, thus increases the uptake [21]. At Cr(III) concentration in solution, 100 mg L^{-1} the adsorption capacity of studied sorbents was almost the same: 27 mg g^{-1} for HAP, 30.5 mg g^{-1} for HAP P123 and 28 mg g^{-1} for HAP F127, respectively.

The isotherms data were analyzed using three commonly used equilibrium models: Langmuir, Freundlich and Temkin. The mathematical expressions of the linear form of applied models are given by Eqs. (8)–(11), respectively:

$$\frac{1}{q_e} = \frac{1}{q_{\max}} + \frac{1}{bq_{\max}C_e} \tag{8}$$

where C_e is metal ions concentration at equilibrium (mg L^{-1}), q_e is the amount of metal adsorbed at equilibrium (mg g^{-1}), $q_{\max}$ is maximum adsorption capacity of the sorbent (mg g^{-1}) and b is Langmuir adsorption constant (L mg^{-1}). K_L is a constant that is important in calculating the dimensional parameter (R_L) that explains the favorability of the adsorption process; R_L is calculated using the equation given below:

$$R_L = \frac{1}{1 + K_L C_0} \tag{9}$$

where $R_L > 1$ the adsorption process is unfavorable; $R_L = 1$ adsorption is linear; $0 < R_L < 1$ adsorption process is favorable; $R_L = 0$ adsorption is irreversible.

$$\ln q_e = \ln K_F + \frac{1}{n}\ln C_e \tag{10}$$

where q_e is the amount of metal adsorbed at equilibrium (mg g^{-1}), C_e is the concentration of metal ions in aqueous solution at equilibrium (mg L^{-1}); K_F and n are Freundlich constants that include factors that affect adsorption capacity and adsorption intensity, respectively.

$$q_e = \frac{RT}{b_T}\ln K_T + \frac{RT}{b_T}\ln C_e \tag{11}$$

where T is the absolute temperature (K), R is the universal gas constant (8.314 J mol^{-1} K^{-1}), K_T is the equilibrium binding constant (L mg^{-1}), and b_T is the variation of adsorption energy (kJ mol^{-1}). B is Temkin constant related to the heat of adsorption (kJ mol^{-1}). In the above equation, $B = RT/b_T$.

The adsorption isotherms for Cr(III) ions adsorption on HAP and its two modifications are presented in Fig. 9.

The coefficients of determination (R^2) and isotherm parameters from the linear regressive method are listed in Table 3.

According to the calculated values of the coefficients of determination, the Freundlich isotherm model represented the poorest fit of experimental data (R^2 0.93 for all sorbents). The isotherm is considered valid for weak van der Waals type adsorption as well as for strong chemisorption [22]. The $1/n$ value calculated from the Freundlich isotherm model was less than unity for all systems, indicating that the adsorption of Cr(III) onto HAP and its two modifications was favorable.

The Langmuir model was found to fit well experimental data for all three analyzed sorbents. The Langmuir isotherm is based on the assumption that uptake occurs on a homogenous surface by monolayer adsorption without interaction between adsorbed molecules [23]. It is suggested that HPO_4^{2-} groups play the main role in Cr(III) ions binding. The maximal theoretical adsorption capacity of analyzed sorbent increased in the following order HAP < HAP P123 < HAP F127. The R_L values between 0 and 1 indicate favorable adsorption. It should be mentioned that the maximum adsorption capacity of HAP treated with pluronic F127 surfactant was approximately two times higher than for the other two sorbents. In Si et al. [3] study it was shown that the Langmuir adsorption isotherm well fitted the adsorption data for the

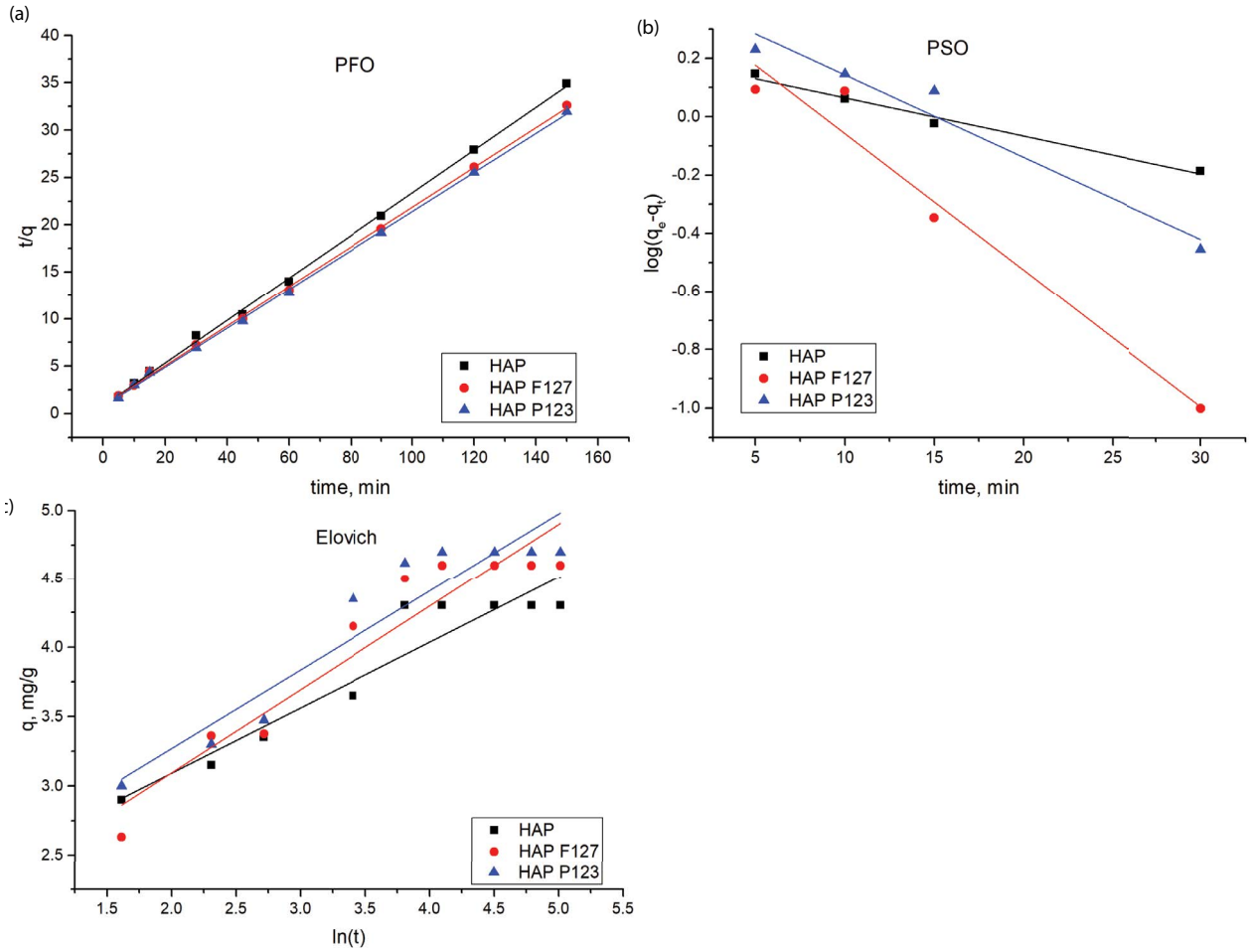

Fig. 6. Kinetics of chromium(III) adsorption on hydroxyapatites: (a) pseudo-first-order, (b) pseudo-second-order and (c) Elovich model.

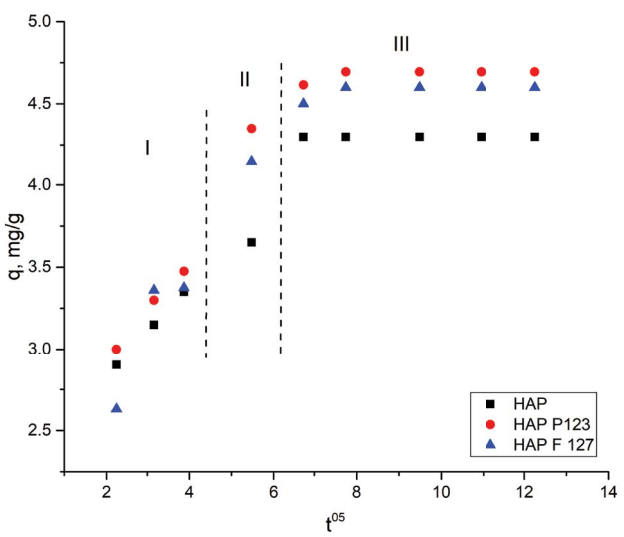

Fig. 7. A plot of intraparticle diffusion modeling of Cr(III) adsorption onto hydroxyapatites.

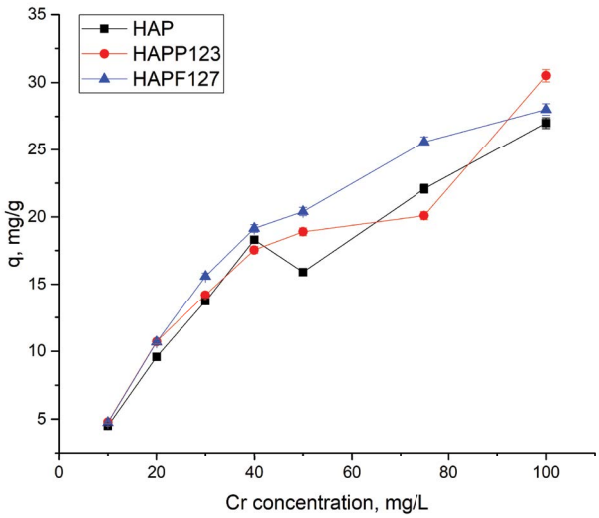

Fig. 8. Adsorption of chromium ions as the function of chromium concentration in solution (temperature 20°C; sorbent dosage 0.02 g; contact time 1 h).

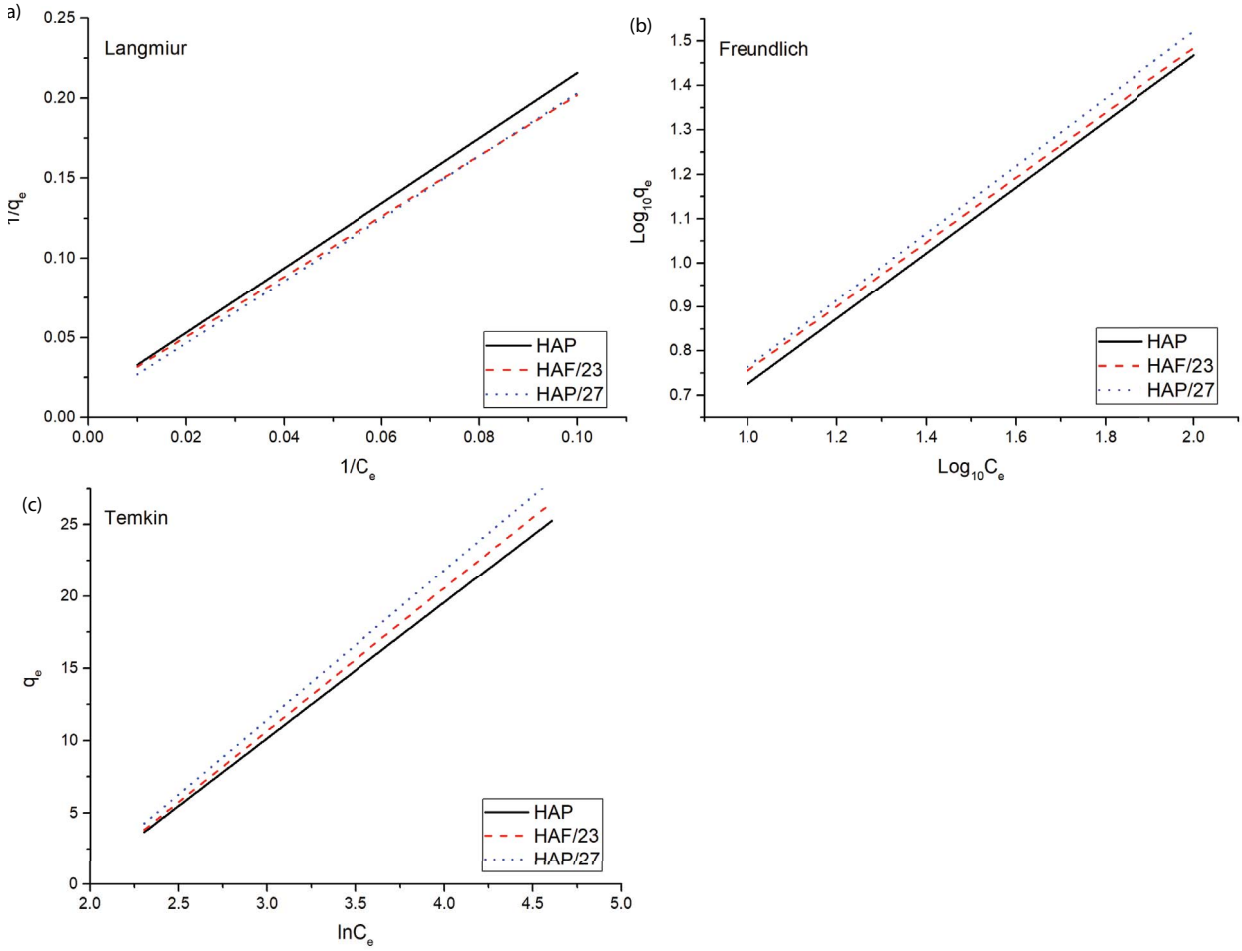

Fig. 9. Isotherm plots of HAP, HAP P123 and HAP F127 adsorbents for Cr(III) removal (a) Langmuir, (b) Freundlich and (c) Temkin.

Table 3
Adsorption isotherm parameters

Model	HAP	HAP F127	HAP P123
q_{exp}	27	28	30.5
Langmuir			
q_{max} (mg g^{-1})	79.7	134.8	78.1
b (L g^{-1})	0.006	0.004	0.007
R_L	0.99	0.99	0.99
R^2	0.98	0.98	0.97
Freundlich			
K_F	0.96	1.01	1.06
$1/n$	0.74	0.77	0.76
R^2	0.93	0.93	0.93
Temkin			
K_T	0.15	0.15	0.15
b_T	0.26	0.23	0.25
B	9.4	10.7	9.9
R^2	0.95	0.99	0.91

adsorption of Cr(III) ions on HAP nanoparticles as compared to the Freundlich adsorption isotherm.

Coefficients calculated for the Temkin model for HAP and HAP F127 were on the level of those obtained for Langmuir models, while for HAP P123 coefficient of determination calculated from the Temkin model was lower (0.91). The Temkin isotherm takes into account the interactions between adsorbents and metal ions to be adsorbed and is based on the assumption that the free energy of adsorption is a function of the surface coverage and adsorption is characterized by a uniform distribution of the binding energies, up to some maximum binding energy [24]. The Temkin constant (B) values related to the heat of adsorption were in the range of 9.4–10.7 kJ mol^{-1}. It has been reported by Ho et al. [25] that the typical range of bonding energy for the ion-exchange mechanism is 8–16 kJ mol^{-1}. The positive value of b_T indicates the endothermic character of Cr(III) ions adsorption.

Comparison of adsorption capacity of the analyzed sorbents and the data obtained for other sorbents are presented in Table 4.

4. Conclusions

Cr(III) adsorption on HAP and its two modifications was studied as a function of pH, Cr(III) concentration and

Table 4
Comparison of adsorption capacity of different sorbents toward chromium(III) ions

Sorbent	pH	q_m, mg g^{-1}	Reference
HAP	5	27	Present study
HAP P123	5	30.5	Present study
HAP F127	5	28	Present study
Bone char	5	78.6	[9]
Activated carbon	5	23	[15]
Animal bones	5	39–194	[8]
Amberlite IR-120 resin	–	67.7	[26]
Jatropha curcas L.	5.5	16	[10]
Vesicular basalt rock	6	0.9	[27]

time of interaction. According to calculated parameters, the adsorption of Cr(III) ions on studied sorbents followed the second-order kinetic model, and the intraparticle diffusion mechanism was the dominating control process. The Langmuir, Freundlich and Temkin adsorption models were used for the mathematical description of the adsorption equilibrium of Cr(III) ions onto sorbents. It was found that the maximum Cr(III) adsorption capacity of analyzed sorbents is 78.1 mg g^{-1} HAP P123, 79.7 mg g^{-1} for HAP and 134 mg g^{-1} for HAP F127. Ion-exchange can be considered the main mechanism of Cr(III) ions adsorption. The obtained data shows that studied sorbents can be efficiently used for Cr(III) ions removal from wastewater. A further economic study will be evaluated in order to assess the efficiency of the preparation of the sorbents based on hydroxyapatite.

Acknowledgment

This work was supported by the IUCN-Dubna project, No. 03–4-1128–2017/2019, theme 100.

References

[1] J.S. Liu, L.L. Wu, X.H. Chen, Kinetic model investigation on lead(II) adsorption using silica-based hybrid membranes, Desal. Water Treat., 54 (2015) 2307–2313.
[2] T.M. Zewail, N.S. Yousef, Kinetic study of heavy metal ions removal by ion exchange in batch conical air spouted bed, Alexandria Eng. J., 54 (2015) 83–90.
[3] Y. Si, J. Huo, H.B. Yin, A. Wang, Adsorption kinetics, isotherms, and thermodynamics of Cr(III), Pb(II), and Cu(II) on porous hydroxyapatite nanoparticles, J. Nanosci. Nanotechnol., 18 (2018) 3484–3491.
[4] P. Miretzky, A. Saralegui, A.F. Cirelli, Simultaneous heavy metal removal mechanism by dead macrophytes, Chemosphere, 62 (2006) 247–254.
[5] I. Mobasherpour, E. Salahi, M. Pazouki, Removal of nickel(II) from aqueous solutions by using nano-crystalline calcium hydroxyapatite, J. Saudi Chem. Soc., 15 (2011) 105–112.
[6] M. Ferri, S. Campisi, M. Scavini, C. Evangelisti, P. Carniti, A. Gervasini, In-depth study of the mechanism of heavy metal trapping on the surface of hydroxyapatite, Appl. Surf. Sci., 475 (2019) 397–409.
[7] Q.Y. Ma, S.J. Traina, T.J. Logan, J.A. Ryan, Effects of aqueous Al, Cd, Cu, Fe(II), Ni, and Zn on Pb immobilization by hydroxyapatite, Environ. Sci. Technol., 28 (1994) 1219–1228.
[8] K. Chojnacka, Equilibrium and kinetic modelling of chromium(III) sorption by animal bones, Chemosphere, 59 (2005) 315–320.
[9] J.V. Flores-Cano, R. Leyva-Ramos, F. Carrasco-Marin, A. Aragón-Piña, J.J. Salazar-Rabago, S. Leyva-Ramos, Adsorption mechanism of chromium(III) from water solution on bone char: effect of operating conditions, Adsorption, 22 (2016) 297–308.
[10] A.C. Gonçalves Jr., H. Nacke, D. Schwantes, M.A. Campagnolo, A.J. Miola, C.R. Teixeira Tarley, D.C. Dragunski, F.A. Cajamarca Suquila, Adsorption mechanism of chromium(III) using biosorbents of *Jatropha curcas* L, Environ. Sci. Pollut. Res., 24 (2017) 21778–21790.
[11] M.S.M. Arsad, P.M. Lee, L.K. Hung, Synthesis and Characterization of Hydroxyapatite Nanoparticles and β-TCP Particles, 2nd International Conference on Biotechnology and Food Science IPCBEE, IACSIT Press, Singapore, 2011, pp. 184–188.
[12] S. Campisi, C. Castellano, A. Gervasini, Tailoring the structural and morphological properties of hydroxyapatite materials to enhance the capture efficiency towards copper(II) and lead(II) ions, New J. Chem., 42 (2018) 4520–4530.
[13] E. Deydier, R. Guilet, P. Sharrock, Beneficial use of meat and bone meal combustion residue: "an efficient low cost material to remove lead from aqueous effluent", J. Hazard. Mater. B, 101 (2003) 55–64.
[14] L.-C. Hsu, Y.-T. Liu, C.-H. Syu, M.-H. Huang, Y.-M. Tzou, H.Y. Teah, Adsorption of tetracycline on Fe (hydr)oxides: effects of pH and metal cation (Cu^{2+}, Zn^{2+} and Al^{3+}) addition in various molar ratios, R. Soc. Open Sci., 5 (2018) 171941.
[15] R. Leyva-Ramos, L. Fuentes-Rubio, R.M. Guerrero-Coronado, J. Mendoza-Barron, Adsorption of trivalent chromium from aqueous solutions onto activated carbon, J. Chem. Technol. Biotechnol., 62 (1995) 64–67.
[16] M. Wakamura, K. Kandori, T. Ishikawa, Surface composition of calcium hydroxyapatite modified with metal ions, Colloids Surf., A, 142 (1998) 107–116.
[17] Y.S. Ho, G. McKay, Pseudo-second-order model for sorption processes, Process Biochem., 34 (1999) 451–465.
[18] N.Y. Mezenner, A. Bensmaili, Kinetics and thermodynamic study of phosphate adsorption on iron hydroxide-eggshell waste, Chem. Eng. J., 147 (2009) 87–96.
[19] M.A. Ahmad, N.A.A. Puad, O.S. Bello, Kinetic, equilibrium and thermodynamic studies of synthetic dye removal using pomegranate peel activated carbon prepared by microwave-induced KOH activation, Water Resour. Ind., 6 (2014) 18–35.
[20] V.O. Shikuku, R. Zanella, C.O. Kowenje, F.F. Donato, N.M.G. Bandeira, O.D. Prestes, Single and binary adsorption of sulfonamide antibiotics onto iron-modified clay: linear and nonlinear isotherms, kinetics, thermodynamics, and mechanistic studies, Appl. Water Sci., 8 (2018) 175.
[21] Z. Aksu, S. Tezer, Biosorption of reactive dyes on the green alga *Chlorella vulgaris*, Process Biochem., 40 (2005) 1347–1361.
[22] F. Ouadjenia-Marouf, R. Marouf, J. Schott, A. Yahiaoui, Removal of Cu(II), Cd(II) and Cr(III) ions from aqueous solution by dam silt, Arabian J. Chem., 6 (2013) 401–406.
[23] N.S. Yousef, R. Farouq, R. Hazzaa, Adsorption kinetics and isotherms for the removal of nickel ions from aqueous solutions by an ion-exchange resin: application of two and three parameter isotherm models, Desal. Water Treat., 57 (2016) 21925–21938.
[24] K.G. Akpomie, F.A. Dawodu, K.O. Adebowale, Mechanism on the sorption of heavy metals from binary-solution by a low cost montmorillonite and its desorption potential, Alexandria Eng. J., 54 (2015) 757–767.
[25] Y.S. Ho, D.A.J. Wase, C.F. Forster, Removal of lead ions from aqueous solution using *Sphagnum* moss peat as adsorbent, Water SA, 22 (1996) 219–224.
[26] F.J. Alguacil, M. Alonso, L.J. Lozano, Chromium(III) recovery from waste acid solution by ion exchange processing using Amberlite IR-120 resin: batch and continuous ion exchange modelling, Chemosphere, 57 (2004) 789–793.
[27] A. Alemu, B. Lemma, N. Gabbiye, K.Y. Foo, Adsorption of chromium(III) from aqueous solution using vesicular basalt rock, Cogent Environ. Sci., 5 (2019) 1650416.